DEVELOPMENT OF A MULTISENSORY SADDLE AS INPUT DEVICE FOR TELEOPERATION

TJARK WELTER (MATR.-NR. 6032630)

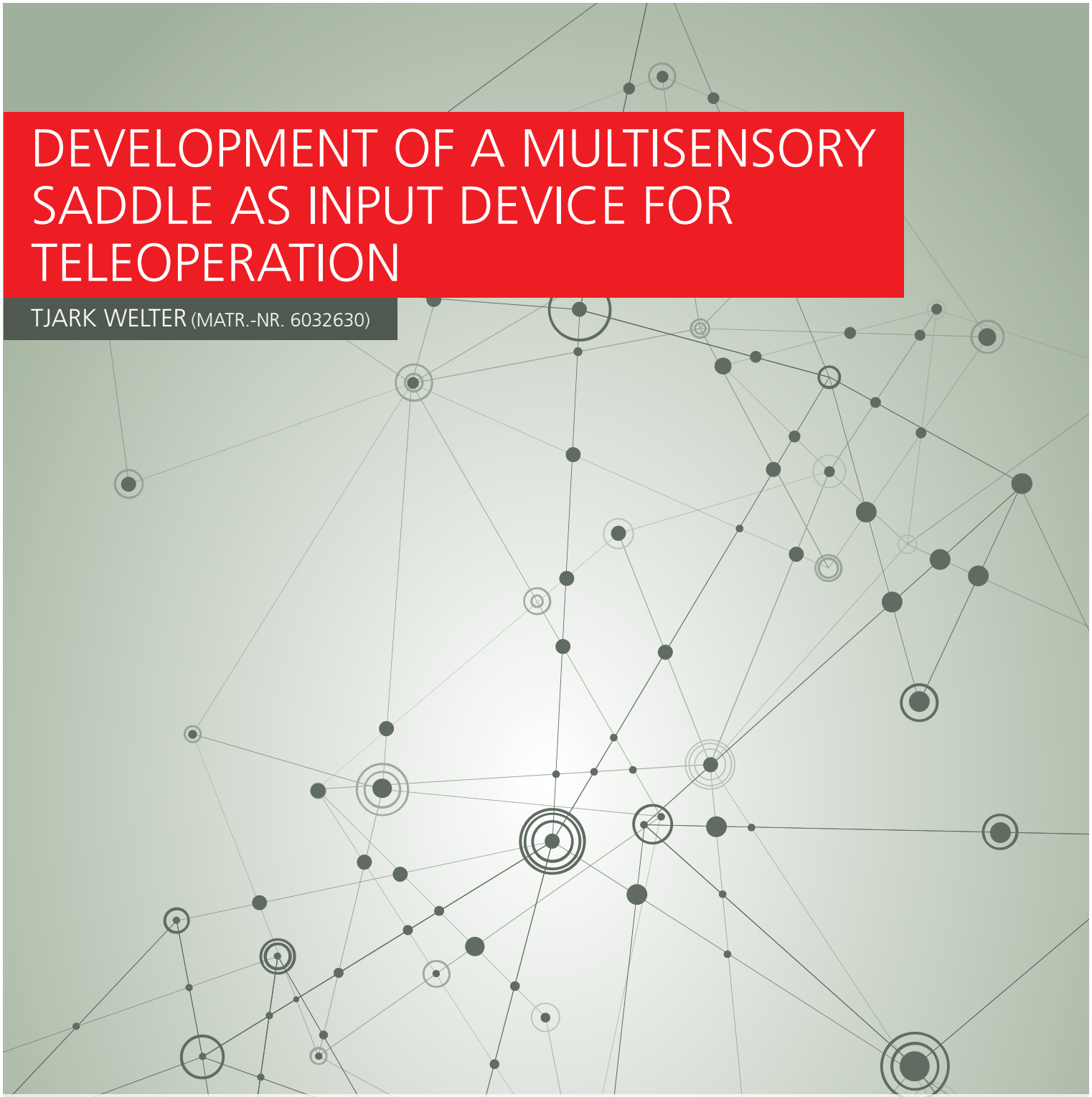

Bachelor's Thesis
16. February 2023

First Examiner
Prof. Dr.-Ing. Frank Wallhoff

Second Examiner
Dr.-Ing. Thomas Hulin

JADE HOCHSCHULE
Wilhelmshaven Oldenburg Elsfleth

DLR

SMiLE

Jade University of Applied Sciences Wilhelmshaven/Oldenburg/Elsfleth
Faculty of Civil Engineering, Geoinformation and Health Technology
Abteilung Technologie und Gesundheit für Menschen
Zeughausstraße 73a
26121 Oldenburg
Germany

Development of a Multisensory Saddle as Input Device for Teleoperation

Tjark Welter
Matr.-Nr. 6032630

Bachelor's Thesis
16. February 2023

First Examiner
Prof. Dr.-Ing. Frank Wallhoff

Second Examiner
Dr.-Ing. Thomas Hulin

Jade University of Applied Sciences Wilhelmshaven/Oldenburg/Elsfleth
Faculty of Civil Engineering, Geoinformation and Health Technology
Abteilung Technologie und Gesundheit für Menschen
Zeughausstraße 73a
26121 Oldenburg
Germany

Starting Date:	22. December 2022
Due Date:	16. February 2023

First Examiner:	Prof. Dr.-Ing. Frank Wallhoff Jade University of Applied Sciences Wilhelmshaven/Oldenburg/Elsfleth Ofener Str. 16/19 26121 Oldenburg Germany
Second Examiner:	Dr.-Ing. Thomas Hulin German Aerospace Center (DLR) Institute for Robotics and Mechatronics Münchener Str. 20 82234 Weßling
Supervisors:	Jörn Vogel and Tilo Wüstenhoff German Aerospace Center (DLR) Institute for Robotics and Mechatronics Münchener Str. 20 82234 Weßling

ABSTRACT

English

Due to demographic change and a skilled labour shortage in healthcare professions it is of high importance to explore technological assistance in healthcare. This thesis aims to develop a multisensory saddle as an additional input device to the HUG (Haptisches User Gerät) to be used for teleoperation in the SMiLE (Servicerobotik für Menschen in Lebenssituationen mit Einschränkungen) ecosystem. Since the HUG's input is limited to two robotic arms, the operator cannot control the mobile platform and the arms of a robot at the same time. Adding the saddle developed in this thesis to the HUG setup will resolve this, allowing the operator to control a robotic platform by pressing sensors with their legs. After evaluating different sensors, a sensor module is developed around a spring-loaded potentiometer, which is placed on the saddle adjustably to account for differences in the operators' height. Following the implementation of the necessary software infrastructure, the saddle will be validated in a user study comparing two different steering approaches: differential driving with and without the additional option to drive sideways. Obtaining mostly positive results about both the functionality to drive sideways and the saddle as an input device from the study thus concludes the development of a first prototype for the saddle.

Deutsch

Aufgrund des demografischen Wandels und des Fachkräftemangels in Pflegeberufen ist es besonders wichtig, technische Möglichkeiten für Unterstützungssysteme für die Pflege zu erforschen. Diese Arbeit hat das Ziel, einen multisensorischen Sattel als zusätzliches Eingabegerät für das HUG (Haptisches User Gerät) zu entwickeln, welches im SMiLE (Servicerobotik für Menschen in Lebenssituationen mit Einschränkungen) Ökosystem für die Teleoperation genutzt wird. Da die Eingabemöglichkeiten des HUGs auf zwei Roboterarme beschränkt sind, kann der Teleoperator nicht gleichzeitig die Fahrplattform und die Arme eines Roboters steuern. Diese Problematik wird mit dem hier entwickelten Sattel behoben, indem dem Teleoperator ermöglicht wird, durch das Drücken von Sensoren mit den Beinen die Fahrplattform zu steuern. Zusätzlich zum Vergleich verschiedener Sensortypen wird ein Sensormodul auf der Basis eines gefederten Potentiometers entwickelt, welches verstellbar am Sattel angebracht wird, um Größenunterschiede der Nutzer ausgleichen zu können. Außerdem wird die nötige Software Infrastruktur implementiert. Zudem wird der Sattel in einer Nutzerstudie evaluiert, die zudem zwei Steuerungsansätze vergleicht: eine differenzielle Steuerung mit und ohne die zusätzliche Möglichkeit, seitwärts zu fahren. Die positiven Ergebnisse der Studie zur Funktionalität des seitwärts Fahrens sowie zum Sattel als Eingabegerät zeigen die Gebrauchstauglichkeit und den praktischen Nutzen des Sattelkonzepts.

Keywords: Teleoperation, Robotics, Healthcare, Input Device

CONTENTS

List of Figures

List of Tables

CHAPTER 1

INTRODUCTION

The combination of demographic change and a shortage of skilled workers in healthcare professions, which is likely to get even worse in the future, shows the importance of exploring technological assistance both actively assisting healthcare workers and increasing the independence of patients which decreases the workload of healthcare personnel.

One project aiming for this is the SMiLE ecosystem (Servicerobotik für Menschen in Lebenssituationen mit Einschränkungen, German for service robotics for people in life situations with restrictions) developed by the Institute of Robotics and Mechatronics of the German Aerospace Center (DLR) (Vogel, Leidner, et al., 2021). The goal is to increase a patient's independence by using different robotic systems. An overview of the ecosystem can be found in figure 1.1. It consists of three robotic systems: EDAN, Justin and the HUG. The electronic daily assistant (EDAN) is a motorized wheelchair equipped with a modified DLR lightweight robot (LWR) in order to increase the independence of people sitting in a wheelchair (Vogel, Hagengruber, et al., 2020). The humanoid robot Justin is a bimanual robot on a holonomic platform (Fuchs et al., 2009). While originally designed for space operations it serves as a personal assistant in the SMiLE ecosystem. The HUG (Haptisches User Gerät, German for haptic user device) is a haptic input device consisting of two LWRs and a VR headset (Hulin et al., 2011). It can be used to control both Justin and EDAN if medical or technological support is needed.

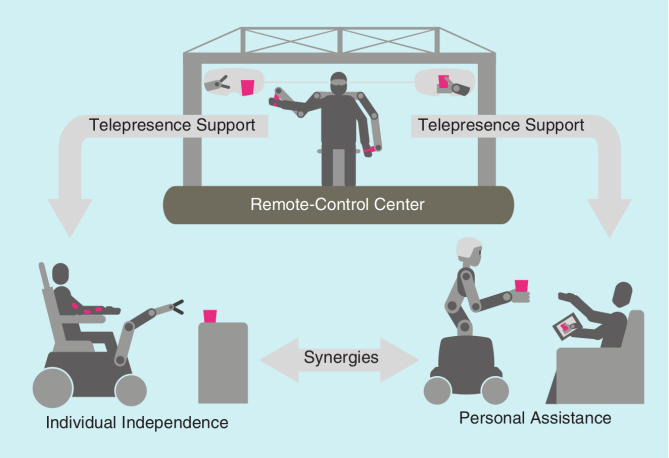

Figure 1.1: The SMiLE Ecosystem consisting of the three robotic systems EDAN (bottom left), Justin (bottom right) and HUG (top) (Vogel, Leidner, et al., 2021).

Figure 1.2: An alternative full-body input device where while the upper body controls are similar to the HUG, the platform is controlled by a so called 3D rudder with the feet. Tilting the rudder leads to the platform moving into that direction while rotation can be invoked by rotating the rudder (Schwarz et al., 2021).

One limitation when using the HUG for teleoperating mobile manipulators is, since the input is limited to the two LWRs, the operator has to choose whether to control the platform or the arms of Justin. One situation where this would be problematic is if Justin is supposed to transport an object that while it is driving also requires regulated grasping, i.e., needs to be held firm enough not to fall but not too firm so it does not break. To solve this problem, a new input device needs to be added to the HUG to take over either controlling the platform or the arms. As the current setup of the HUG was designed with a focus on bimanual teleoperation, the new input device would need to control Justin's platform. And since the upper body of the operator is already busy controlling the arms, the input device needs to be operated with the legs. An alternative design of an input device which has this feature is the input device by Schwarz et al. (Schwarz et al., 2021) as seen in figure 1.2.

Another approach towards an input device will be developed in this thesis. Contrary to the design by Schwarz et al. (Schwarz et al., 2021) this input device will be a multisensory saddle on which the operator sits similarly to sitting on a horse or motorcycle (as seen in figure 1.3). While sitting, they control four sensors with their knees and feet, which are then interpreted to yield motion of the platform. Covering the development process of the first prototype of this input device, this thesis is structured as follows: After this introduction, the important theoretical background is explained in chapter 2. This includes some basics on teleoperation as well as covering steering approaches for mobile platforms and the M5Core2 microcontroller used. In order to equip the saddle with sensors, those to be used have to be chosen first. Therefore, requirements for the sensors are determined in chapter 3. Then possible sensors are evaluated and tested on the prototype. Once the sensors are chosen, the sensor modules are designed. Their design is explained in chapter 4. This includes the design of sensor modules for the sensors selected to be tested on the

Figure 1.3: A concept drawing of a “total HUG”, a combination of the HUG and a saddle (Wüstenhoff, n.d.).

prototype in chapter 3 as well as the placement of the sensor modules on the saddle. Chapter 5 covers the implementation of the software infrastructure used in the prototype, from reading the sensor data to processing and interpreting it. Based on the hardware from chapter 4 and the software from chapter 5, the final prototype is validated with a user study in chapter 6. The chapter goes over the design of the study and then presents the results. Finally, the development process is summarized in chapter 7. Additionally, an overview over future work on the prototype is given.

CHAPTER 2

THEORETICAL BACKGROUND

This chapter covers the theoretical information needed for the development of the prototype. Starting by explaining the basics of teleoperation, it will then discuss different approaches for steering mobile platforms, followed by a description of some of the hardware components used.

2.1 Basics of Teleoperation

Teleoperation describes the process of controlling for example a robot from a distance. Because the field is quite extensive, this section will only cover the basics needed for this development process.

According to Niemeyer et al. (Niemeyer et al., 2016) the goal of teleoperation is to let the operator "not only [...] manipulate the remote environment, but also [...] perceive the environment as if encountered directly." A system achieving this is called transparent. Partial transparency can be achieved through several modalities, mostly connected to the human senses. While a bilateral communication between input device and robot is needed for most of these modalities, i.e., visual or force feedback, designing an input device in a way to give the user feedback on the current input given can also help.

2.2 Steering Approaches for Mobile Platforms

While there is a variety of kinematics for robotic platforms, this section will describe only differential and holonomic driving, as these represent the kinematics of the robotic systems the input device is mainly designed for.

As described by LaValle (LaValle, 2013), differential drives consist of two non-steerable but separately controllable wheels. Additionally, caster wheels can be added for balance. Because both wheels can be rotated separately, a robot with a differential drive can not only drive forward, backwards and curves but also rotate on the spot.

Meanwhile, holonomic locomotion in regards of mobile robotic platforms means that the plat-

form is also able to drive sideways. This can be achieved by using special wheels like the mecanum wheels discussed by Zeidis and Zimmermann (Zeidis and Zimmermann, 2019) or by adding a steering drive capable of rotating the vertical axis of the wheels, as done in the platform of Rollin' Justin (Fuchs et al., 2009).

2.3 The M5Core2 Microcontroller

The M5Core2 (further called M5) is the second generation of the Core microcontroller by M5Stack. It is equipped with an ESP32 chip, built-in touchscreen and battery, a USB TypeC port, a GROVE port (which can be used for input-output (I/O) or inter-integrated circuit (I2C) communication) and many more features (M5Stack, n.d.[c]). While it only has two analog-to-digital converters (ADC), a so-called Port-B Hub (PbHub) by M5Stack can be connected via I2C to communicate with up to six more analog devices (M5Stack, n.d.[b]).

CHAPTER 3

CHOOSING THE SENSORS TO BE USED

Before the prototype can be equipped with sensor modules, the appropriate sensors need to be chosen. This chapter explains their requirements, which sensors are considered and the final choice.

3.1 Requirements for the Sensors

The requirements for the sensors can be derived from the concept of the input device. The general idea for the device is for the operator to be able to control a mobile platform with their legs, or more precisely via four inputs: one at each knee and foot. Therefore, the sensors need to be able to accurately measure either a change in position (rotational or translational) of the knee or foot or the force applied by them. Additionally, their data rate needs to be fast enough for the latency between input and robot action not to interfere with a safe and precise operation of the robot. This results in the following criteria to evaluate which sensors to choose:

- Accuracy
- Sampling frequency
- Controllability

Two further aspects considered in the evaluation of the sensors are the complexity of designing a sensor module with them and whether they provide some sort of feedback to the operator. While these two aspects are both valid, they are not as important as the others, since the problems they raise can be solved comparatively easy.

3.2 Evaluation of Possible Sensors

Based on these criteria, several sensors are evaluated. The technical specifications of the evaluated sensors can be found in table 3.1. Simple tests where the sensor values are displayed on the M5 screen show that in terms of latency, subjective accuracy and controllability most sensors

Table 3.1: Technical Specifications of the evaluated sensors. The values are based on the information found in the cited datasheets. As the sampling frequency for analog sensors depends on the analog-to-digital converter (ADC), these sensors only say "analog" in the column for the sampling frequency. As the datasheet for the Magnetic Rotary Position Sensor stats that the data rate is only limited by the speed of the I2C-connection, it says "I2C" in the column for sampling frequency. Some datasheets did not specify an accuracy of the sensor, which is why it is subjectively evaluated, as described in section 3.2.

Sensor	Range (Accuracy)	Sampling Frequency
Time of Flight (ToF) (M5Stack, n.d.[d])	$0.3 - 2\,\text{m}$ ($\pm 3\,\%$)	$5\,\text{Hz}$
Force Sensing Resistor (FSR) (Ohmite, 2018)	$0.2 - 50\,\text{N}$ ($\pm 6\,\%$)	analog
Magnetic Rotary Position Sensor (Seeed Technology, n.d.)	0 - 4095 ($\pm 0.5\,\%$)	I2C
Rotary Potentiometer (M5Stack, n.d.[a])	$0 - 10\,\text{k}\Omega$ / $0 - 300°$	analog
Linear Potentiometer (M5Stack, n.d.[e])[1](Bourns, 2015)[2]	$0 - 10\,\text{k}\Omega$ / $0 - 35\,\text{mm}$[1] $0 - 10\,\text{k}\Omega$ / $0 - 35\,\text{mm}$[2]	analog
Load Cell with HX711 as ADC (TE Connectivity Company, 2020; M5Stack, n.d.[f])	$0 - 450\,\text{N}$	$10\,\text{Hz}$

should not be considered.

The load cell has quite a big drift which is rather irregular and therefore difficult to compensate. Also, it needs to be calibrated every time the sensor is powered and the calibration needs to happen in a horizontal position, which would mean that each sensor would need to be taken off the saddle, calibrated and reattached each time the device is used, which is very impractical. Also it turns out to be much slower than said in the datasheet, with data rates around $0.1\,\text{Hz}$.

As for the sensors measuring rotational position changes, integrating them into the saddle would be quite complicated. Due to the rotational axis of the knee going through the hip, it would be difficult to transfer the rotation onto the saddle.

This leaves the linear potentiometer and the time-of-flight sensor for measuring translatory changes and the force sensing resistor (FSR) for measuring forces. While the potentiometer and the time-of-flight sensor measure the same change, the potentiometer has the advantage of giving physical feedback of its current position. Therefore, the potentiometer and the FSR are chosen for further evaluation by testing them on the saddle. While two different potentiometers were tested (the fader module by M5Stack (M5Stack, n.d.[e]) and the PTA4543 by Bourns (Bourns, 2015)), the PTA4543 is chosen for further evaluation, because it has $10\,\text{mm}$ more stroke length (45 rather than $35\,\text{mm}$) and it is not yet integrated into a housing which makes designing a sensor module around it easier.

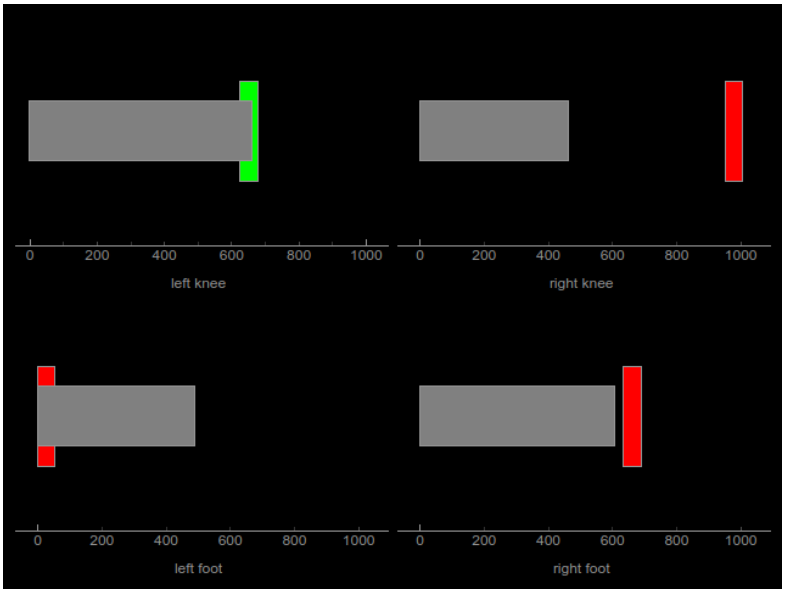

Figure 3.1: The GUI for testing the sensors on the saddle. All four sensors' values are shown as bar graphs. In random intervals, one of the red target areas moves and gets smaller. If a sensor's value matches the target area, the area turns green. The GUI can also be adjusted to showing only one sensor instead of all four.

3.3 Testing Sensors on the Saddle Prototype

To evaluate which sensor is better suited for the input device, both the potentiometer and the FSR are tested on the saddle. In these tests both sensors are attached to the saddle as part of the sensor modules described in chapter 4. Also, the software infrastructure described in chapter 5 is used.

For these tests, either a sensor module with a potentiometer or a FSR is attached to the saddle at the knee or foot position on one side. To reduce the complexity of the testing and allow the operator to focus on one sensor, these tests are conducted with only one sensor at a time. The sensor values are converted to digital through the PbHub and read by the M5 by running the script *m5_sensordata.ino*, which also sends the data to the PC via USB (for more information regarding the software infrastructure see chapter 5). On the PC, a simple program (*saddle_sensor_test.py*) shows the values of the sensor as well as a target value to be matched by the operator. A screenshot of this GUI can be seen in figure 3.1. The program also logs the sensor and target values. Two example plots of these logs can be found in figure 3.2.

As can be seen in the plots, the targets are hit rather consistently with the potentiometer. Meanwhile, trying to match the target value with the FSR seems to be harder, as it is more difficult to control the exact force applied to the sensor. Additionally, the FSR range of 0 to 50 N seems to be wrong, as touching the sensor sometimes leads to the value spiking to the maximum. Therefore, the potentiometer is chosen as the sensor to be used for the sensor modules.

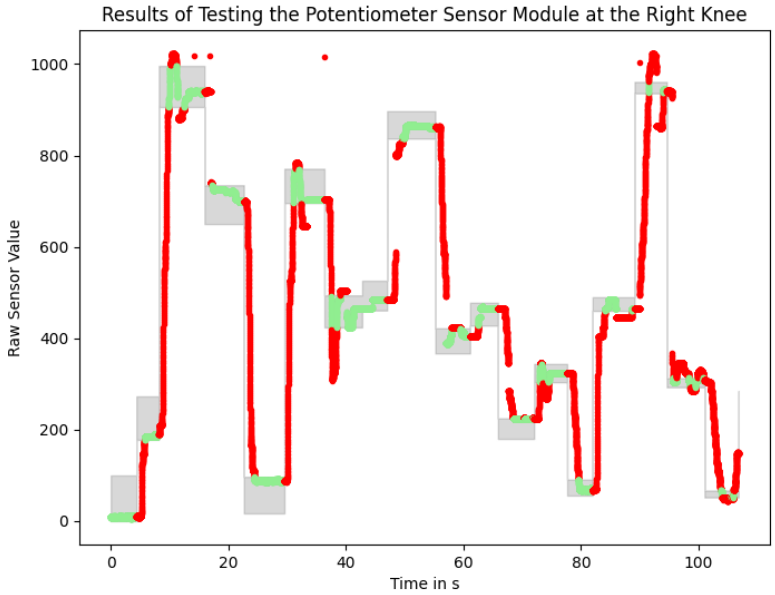

(a) Potentiometer

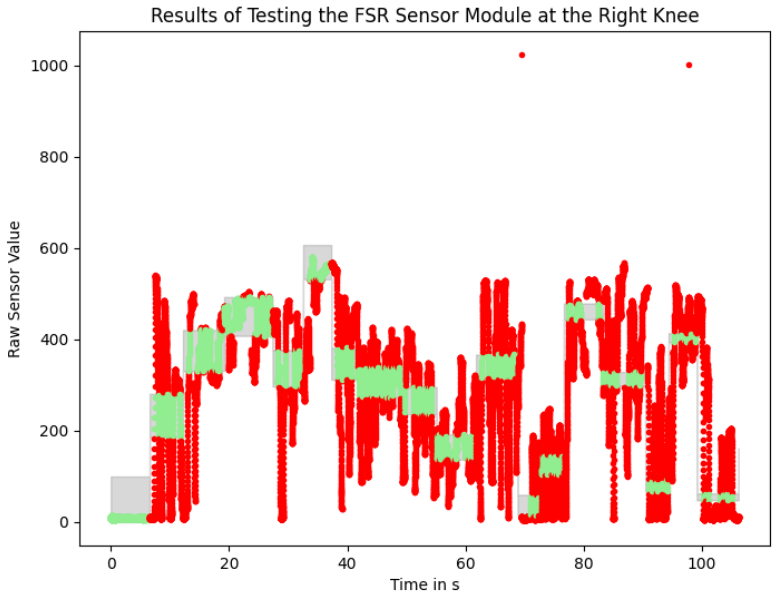

(b) FSR

Figure 3.2: Plot of the sensor values for testing the sensors on the saddle. The grey areas show the target area to be matched and the points the sensor values. Green points indicate the target being hit, red points the target being missed. The plots show the data of the sensors being tested at the right knee position. Because the FSR has a lower resolution with a maximum value of 650, the targets are also only in that range. For better comparison with the data from the potentiometer the y-axis was still scaled to the same range.

CHAPTER 4

DESIGN OF THE SENSOR MODULE

The following chapter deals with the design of the sensor module. At first the design of the sensor module for the FSR is described. Even though this module is not used in the final design for the prototype of the input device, it was used in the testing on the saddle in section 3.3. Thereafter the design of the sensor module with the potentiometer is described and the design process will be explained more thoroughly, starting with the general concept of the module, followed by the choice of spring to be used in the module and the description of the module used in the final prototype. Finally, the placement of the sensors is described.

4.1 FSR Sensor Module Design

As mentioned above, while this module will not be used on the final prototype, it is crucial for the testing that led to the decision which sensor to use (see section 3.3). The requirements for this module are rather simple: It needs to hold both the FSR and its circuit board and provide a way to be attached to the saddle. Also, especially for the knee sensors, it is better for the FSR's sensing surface to have some distance to the saddle, as the corner of the prototype does not allow the operator to bring their knees all the way to the saddle's side panel. These requirements lead to the sensor module design as seen in figure 4.1.

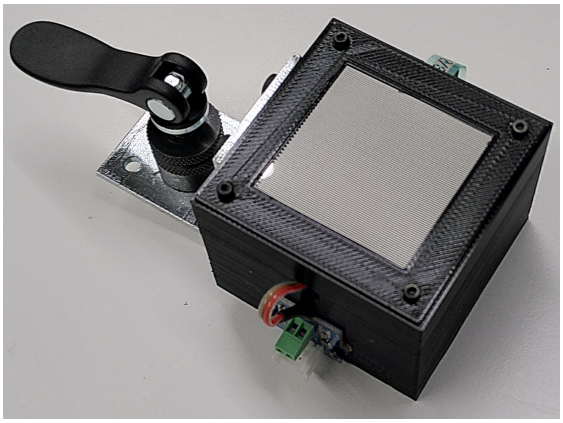

Figure 4.1: The FSR sensor module

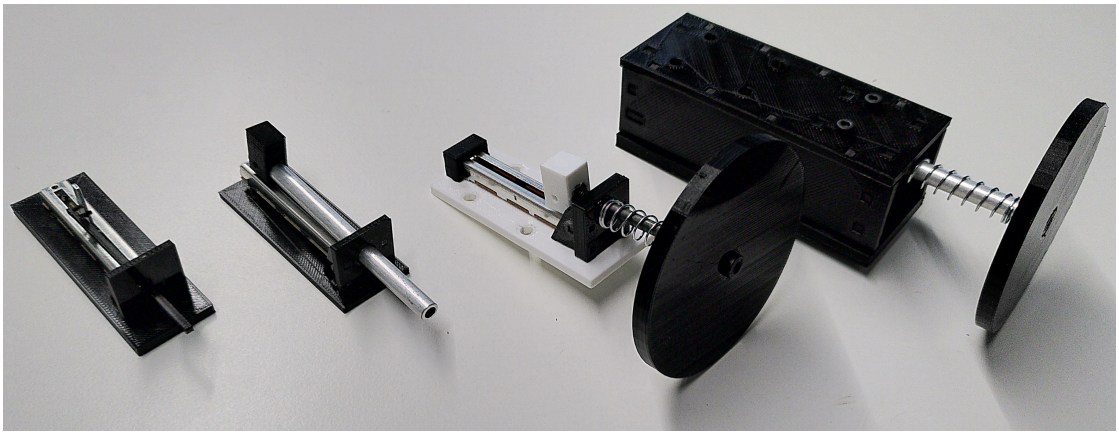

Figure 4.2: The first iterations of the design for the potentiometer sensor module, starting on the left with the first mockup of the overall idea up to the first functional prototype on the right.

4.2 Spring-Loaded Potentiometer Sensor Module Design

For the sensor module with the potentiometer, the concept is somewhat complicated. While the basic requirements remain the same, there is another one that needs to be fullfilled: The module needs to provide a way to transfer the positional change from the leg to the lever of the potentiometer. In the following, the concept for the module is explained, followed by the choice of which spring to use. After that, the final design of the sensor module is presented.

4.2.1 Concept for a Spring Loaded Potentiometer

The basic idea to transfer the positional change is rather simple. There will be some sort of rod connected to the lever of the potentiometer. That way, if the leg pushes the rod, the lever moves and the resistance of the potentiometer changes. A mockup of this idea can be seen in figure 4.2 on the left.

This design has three crucial components: the rod, the part connecting the rod to the lever and a spring to move rod and lever back to their zero position if no force is applied. For the rod a simple aluminum hollow rod is used. This way a thread can be cut into the ends to provide the option to attach things to the rod with screws. These things attached to the rod are a plate to provide better contact to the leg on the one side and the part connecting rod and lever on the other side. The connection part is also screwed to the lever, resulting in a rigid connection between potentiometer and rod.

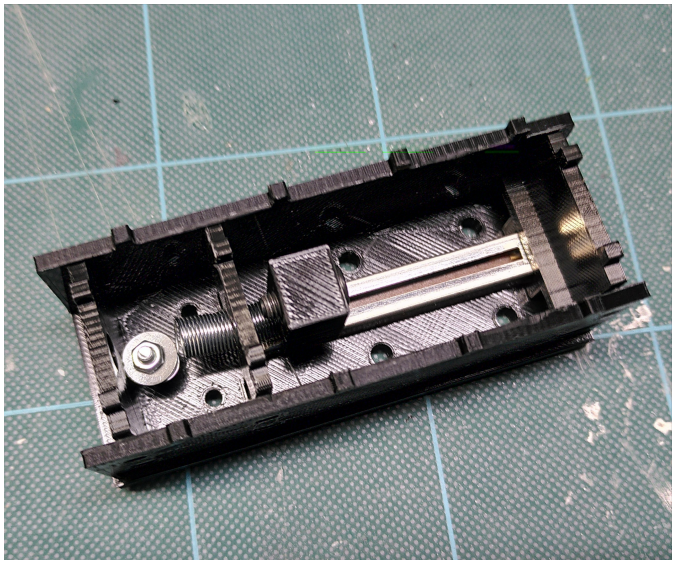

Figure 4.3: The integration of an extension spring into the sensor module. The spring is fixed to the module's floor on the left and to the lever on the right. If the rod (not shown, would enter the module from the left) is pushed, the lever moves right, creating tension on the spring. Once the rod is released, the spring pulls the lever back to its zero position.

4.2.2 Choosing a Spring for the Sensor Module

The third crucial component of the module is a spring. The spring can be integrated in two different ways: as an extension spring between the lever and the front side of the module (as seen in figure 4.3) or as a compression spring between the front side of the module and the plate at the front of the rod (as seen in figure 4.4). While the extension spring has the advantages of being protected inside the module's casing, the only way to avoid friction between the second wall inside the module and the spring is to make the hole inside that wall big enough, which eliminates its purpose as it is meant to guide the rod in order to minimize play in the construction. Therefore, a compression spring is used in the sensor module. Testing with several different springs led to the decision to use the compression spring *D-090G* from Gutekunst (Gutekunst Spring Factories, 2023) with a maximum deflection of $52.9\,\mathrm{mm}$ and a spring rate of $9.5\,\mathrm{N\,mm^{-1}}$. This way the spring is not too strong, thus ensuring long use of the input device without the legs getting tired. Also, the spring is always slightly compressed, as the stroke length of the potentiometer is less than the fully uncompressed spring.

4.2.3 Final Design of the Spring-Loaded Potentiometer Sensor Module

The design of the module went through several iterations, tests and design adjustments. An overview of the designs from the first mockup to the final design can be seen in figure 4.5. One

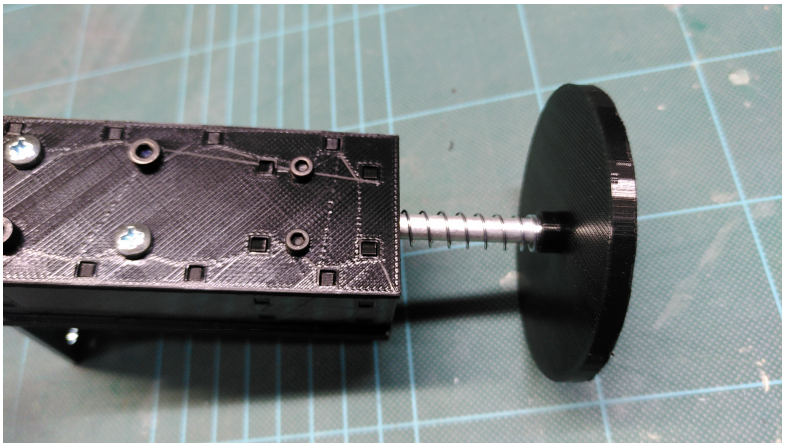

Figure 4.4: The integration of a compression spring into the sensor module. The spring sits between the plate at the end of the rod and the front plate of the module. If the rod is pushed in, the spring is compressed. Once the rod is released, the spring pushes the plate out and thereby also moves the lever back to its zero position.

of the biggest changes is rather apparent from that lineup: the fourth design from the left is the first with a box-like design. This has the advantages of both protecting the potentiometer from outside influences and making the module more robust and stable. A second important change from the first mockup came with it, but cannot be seen from the outside: inside the box is a second front wall. The purpose of this is to provide more stability to the rod, as it is guided by the two front walls. Also, later iterations feature a cylinder coming out of the front wall to provide even more guidance to the rod. A third major change is regarding the plate the leg presses against. In the final design (which can be seen in figures 4.6 and A.2) it is both thicker and includes a socket for the rod to provide more robustness, especially when the operator does not press against the center of the plate.

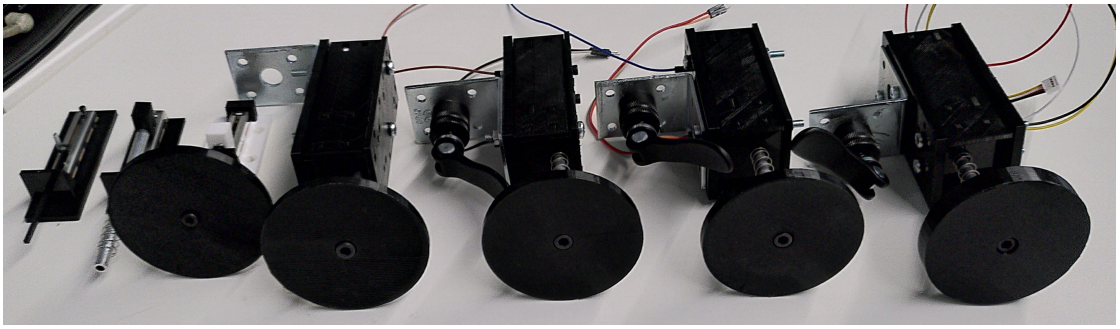

Figure 4.5: Overview of the different designs of the potentiometer sensor module, from the first mockup to the final design.

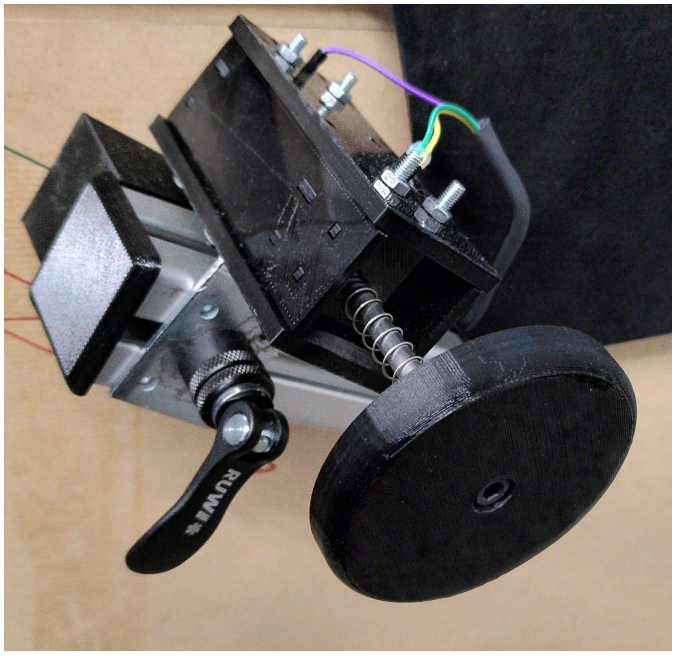

Figure 4.6: The final sensor module mounted on the saddle.

4.3 Placement of the Sensor Modules on the Saddle

Another aspect that influenced the design of the sensor modules is how and where to attach them to the saddle. These positions need to be comfortably accessible by the knees or feet in order to ensure that the operator can use the device safely for long periods of time without it being uncomfortable or even unsafe for example due to unwanted inputs as a result of cramps. While the first module prototypes were simply screwed to the saddle using angular mounting brackets, the final prototype needs to provide a way for the operator to adjust the sensor positioning to their needs.

In order to ensure a comfortable module positioning for the majority of possible operators, the human body dimensions from Ergonomics Standards Committee (Ergonomics Standards Committee, 2020) are used. More specifically, the values from tables 26, 27, 29, 30, 34 and 62 containing the lengths of the upper and lower leg (both with and without the knee) as well as the width of the hip while sitting and the length of the foot are used. From these tables, the fifth percentile of the women is used as the lower border and the 95th percentile of the men as the upper border. From these values, the shortest and longest considered leg are drawn into a 3D-model of the saddle in order to determine along which axes the modules need to be able to be adjusted. This conceptual sketch can be found in figure 4.7. Along the resulting axes ITEM profiles are placed, onto which the sensor modules are fixed with quick-release clamps to provide easy adjusting of the sensors.

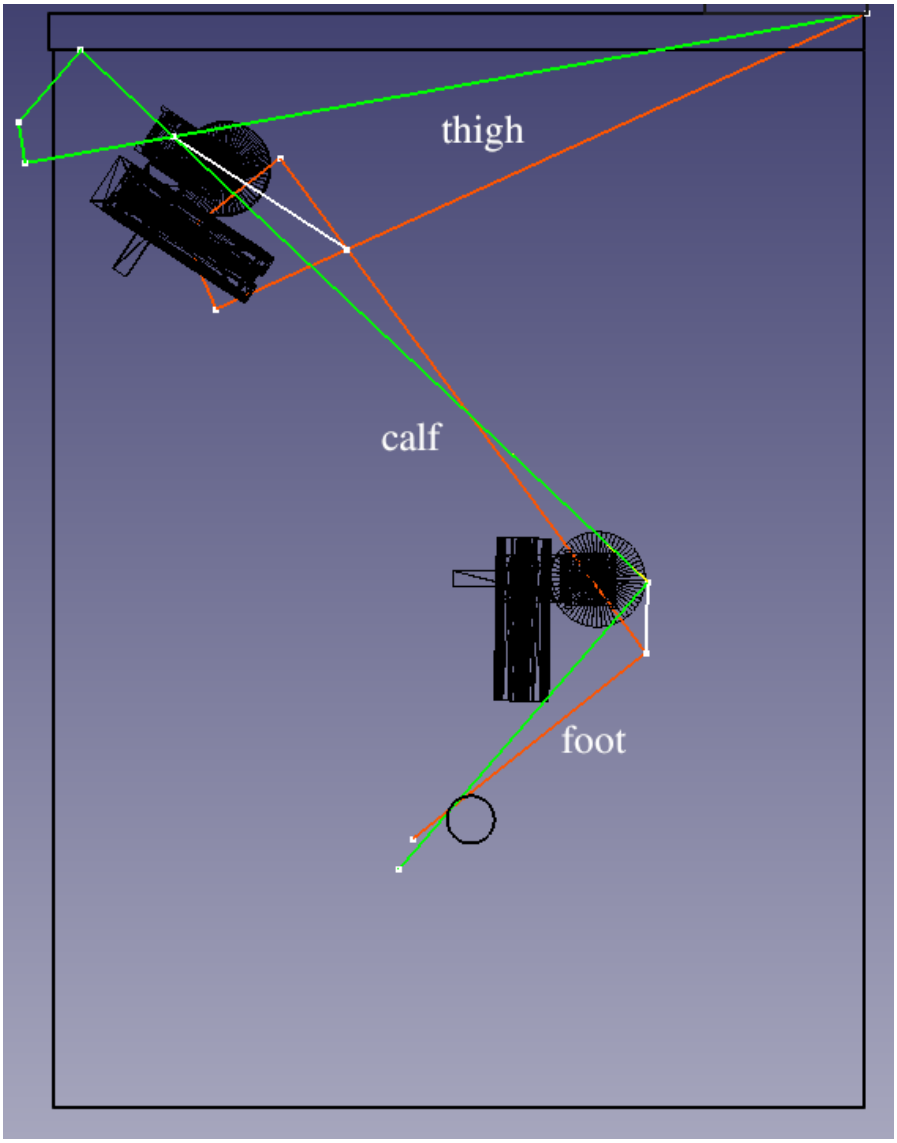

Figure 4.7: Conceptual sketch of the side of the saddle to figure out along which axes the sensor modules should be adjustable. The green lines represent the longest considered leg based on the 95th percentile of the male values from Ergonomics Standards Committee (Ergonomics Standards Committee, 2020), the red lines the shortest considered leg based on the fifth percentile of the female values. The white lines are the resulting axes along which the modules need to be adjustable.

As the operator does not press the knee sensors perpendicular to the saddle side, an angle needs to be put behind the ITEM profiles for the knee sensors to compensate for this. As the angle at which the sensor is pressed is the angle between the thigh and the side of the saddle, it can be calculated with the equation

$$\alpha = \arctan \frac{l_S}{l_T} \tag{4.1}$$

where l_S is the total length of the sensor module and l_T the length of the thigh. Since the sensor should be pressed perpendicular to the leg, there is a right angle between the cathetes l_S and l_T. Using the values from table 29 of Ergonomics Standards Committee (Ergonomics Standards Committee, 2020) for l_T results in a range from

$$\alpha = \arctan \frac{143\,\text{mm}}{435\,\text{mm}} = 18.2^\circ \quad \text{to } \alpha = \arctan \frac{143\,\text{mm}}{540\,\text{mm}} = 14.8^\circ \tag{4.2}$$

for the angle. As the range is not too big and making the angle adjustable would make the design much more complicated, the ITEM profile for the knee sensors will be tilted from the saddle at an angle of 17°.

CHAPTER 5

IMPLEMENTATION OF THE SOFTWARE INFRASTRUCTURE

Besides designing the sensor module, another important step in the development of the prototype is implementing a software infrastructure. In regards to software, the saddle basically consists of two systems: the M5, which is responsible for data acquisition, and the computer, which processes the data it receives from the M5. This chapter explains the software running on these two systems.

5.1 Data Acquisition with the M5

The saddle is equipped with a microcontroller, i.e. the M5. It is responsible for recording the data of the four potentiometers and sending them to the computer via USB. It also shows the sensor values on its display to provide the user with visual feedback on what raw inputs they are giving. Since the M5 only has two ADC-pins, the Port B extension hub (PbHub) is used. This hub can be connected with up to six analog sensors and sends the digitalized data to the M5 via I2C.

In order to create a smooth experience for the operator, it is important to provide the newest sensor values in short and regular intervals. Therefore, the script running on the M5 is split into three separate parts each running on their own thread: reading new sensor values, sending the newest sensor values to the computer and updating the display. While the sensor values are read as quickly as they are available by cycling through the four used ports on the PbHub, the other two threads are run at specific frequencies. This is done by using the *Ticker*-class which can be obtained through the *Ticker*-library provided by the M5's manufacturer M5Stack. An object of this class can be given a method to run and a frequency to run that method and then handles the thread management. One *Ticker*-object is used to send the newest data to the computer with a frequency of 200 Hz and another one to update the display with a frequency of 10 Hz. The 200 Hz for sending the value are used because the PbHub can provide a new value with approximately 1 kHz, which results in a frequency of about 250 Hz for getting a new value from every sensor, as only one sensor can be read from the PbHub at a time. Because updating the display occupies some processing power resulting in a lower frequency for newly obtained sensor values, 200 Hz is chosen as a both stable and high enough frequency to ensure a barely noticeable delay for the operator even after filtering and interpreting the values. Meanwhile, the display is only updated

with 10 Hz to reduce its consumption of processing power and because this is still reasonably fast for the operator to see the current values on the screen.

5.2 Data Processing

On the computer the processing of the data can be divided into three separate steps: receiving the data, preprocessing and interpretation of the data. In the following, these three steps are explained.

5.2.1 Receiving the Data

The computer receives a data packet containing one value for each sensor every 5 ms. This is handled by the so-called data publisher. As the USB connection is prone to corruption and loss of packages, the publisher needs to be designed as robust as possible to ensure safe operation with the prototype. For this, several fail safes are implemented, including throwing errors when the connection is lost and trying to reconnect to the M5 automatically. Another feature for this is an end-of-message flag which is added to the end of every data packet sent by the M5 and checked by the publisher to ensure that the whole packet arrived. If the packet is complete and contains four sensor values within the expected value range, the values are published to links and nodes (LN), a system deployment software developed by the Institute for Robotics and Mechatronics of the German Aerospace Institute. LN provides easy control over processes and communication between different platforms. For the scope of this project it is sufficient to think of LN as a means to share data between different processes.

5.2.2 Data Preprocessing

Before the raw sensor values can be used, they need to be preprocessed in order to eliminate noise (mainly coming from the ADC). Therefore, the data packets published in LN by the publisher are read by a simulink model (see figure 5.1). Afterwards they go through a dead zone and a median filter with a window length of 11 samples. The dead zone (which is set to 50) cuts out the base noise of the ADC when the sensors are in zero position, which is usually between 8 and 24. Additionally, it avoids misinterpreting a touched sensor as pressed because the threshold of 50 has to be surpassed. The median filter is chosen as it is more practical in this situation because the input signal does not have any periodicity but can rather be seen as a changing constant, meaning that within a small time window it will be a constant but from one window to another it might change its value. A window length of 11 samples proves to be long enough to filter out most of the noise while being short enough not to cause too much delay.

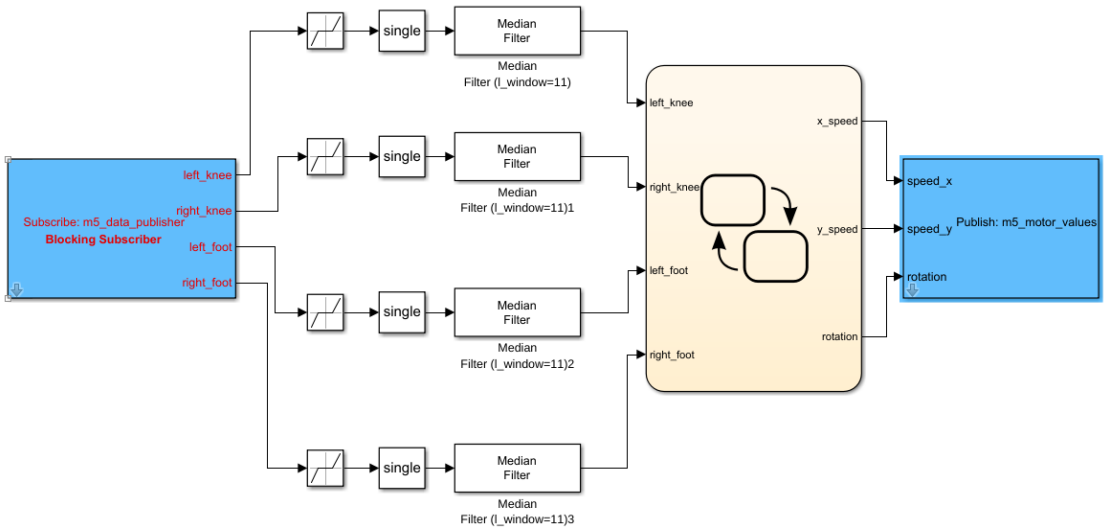

Figure 5.1: The simulink model where the raw sensor values are filtered and interpreted. The resulting movement values are then published to LN.

5.2.3 Data Interpretation

The filtered data is interpreted by state machine (see figure 5.2) based on the steering approaches designed for the saddle. Basically, there are two different approaches: differential driving and holonomic driving. Each approach maps the sensors to specific actions. The mappings are designed to be rather intuitive. Therefore, pressing the two knee sensors moves the platform forward, because they are further to the front of the saddle than the foot sensors. As for rotation and sideways movement, the mappings represent what would happen if the saddle responded to the force applied by the operator, i.e., if it was pressed on the right side, it would move left. An overview of the input-action-mappings can be found in figure 5.3. In addition to the basic actions shown in that overview it is also possible to combine two actions. For example, if both knee sensors and the right foot sensor are pressed for differential driving this would result in the platform driving a forward right curve as a combination of driving forward (because of the knees) and a clockwise rotation (because of the left knee and the right foot). For holonomic driving this would be driving diagonally to the front left, as both sensors on the right being pushed moves the platform to the left. Thus, differential or holonomic driving can be fully implemented with the added safety feature that the platform only moves if at least two and no more than three sensors are being pressed. Accidently pressing one sensor does not lead to the platform moving and pressing all four sensors can be used as an emergency stop.

The state machine returns movement values for the three different driving modes forward (in y-direction), sideways (in x-direction) and rotation. It always takes the lower value of the two sensors responsible for the movement both as a safety feature not to accidently accelerate quickly and to avoid sudden speed changes. The values then get published in LN so that other applications

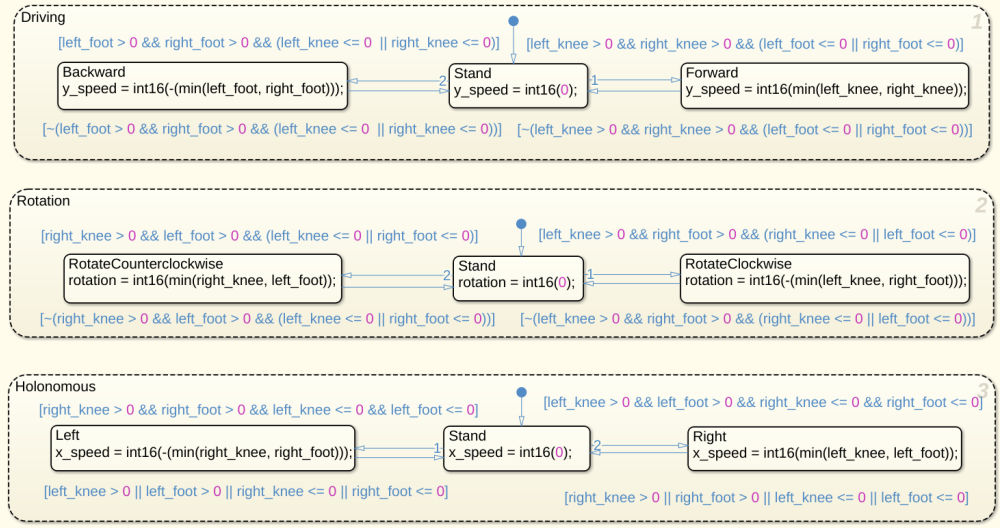

Figure 5.2: The state machine responsible for interpreting the filtered sensor data. It consists of three parallel state machines: one for driving forward or backward, one for rotation and one for driving sideways. The state machines are based on the steering approaches explained in section 5.2.3. If one state is active, i.e., driving forward, the smaller sensor value of the two sensors responsible for this state (i.e., the two knee sensors) is published as the forward movement value which can be mapped to a forward speed.

(simulations or robotic platforms) can use those values and map them to the desired range. The way the state machine in figure 5.2 is implemented, it allows both differential steering by only using the values for forward movement and rotation or a fusion of differential and holonomic driving, where the platform can drive sideways but not diagonally, as pressing three sensors is interpreted as a combination of forward movement and rotation rather than forward and sideways movement.

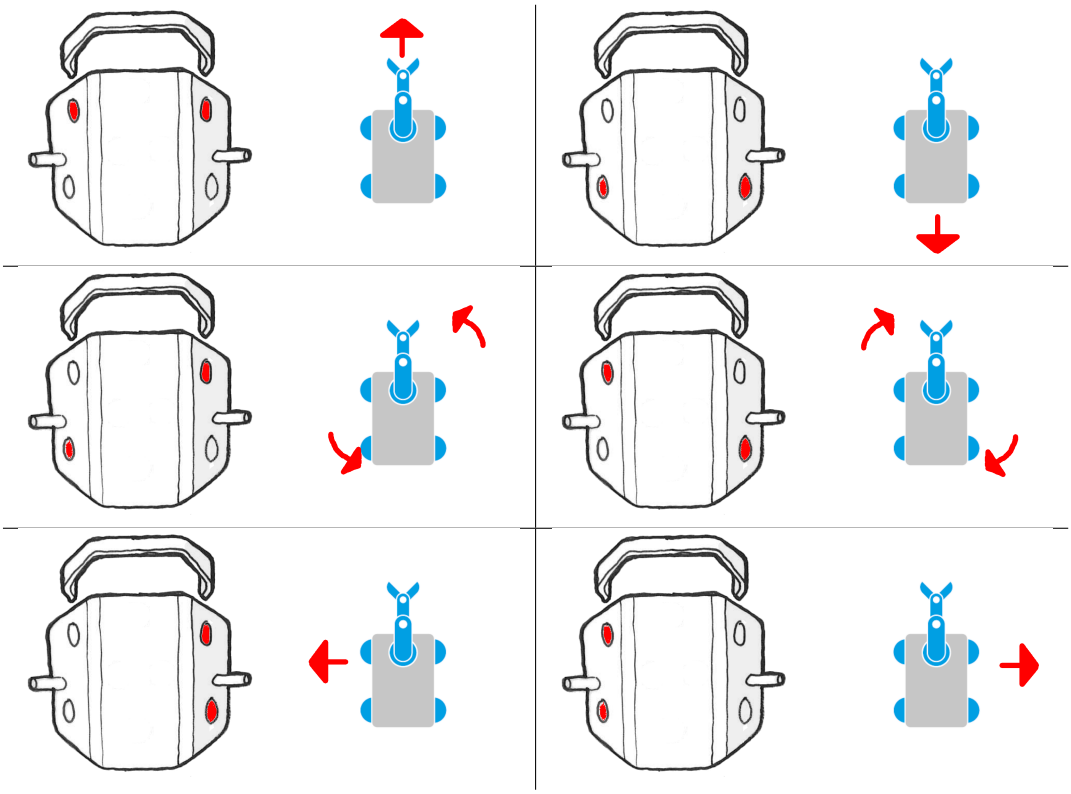

Figure 5.3: Overview over the basic input-action-mappings. On the left of each image the saddle is shown in a top-down view with the pressed sensors colored red. On the right side the resulting movement is displayed.

CHAPTER 6

VALIDATION OF THE PROTOTYPE WITH A USER STUDY

In order to validate the saddle prototype as a usable input device, a user study is conducted. This chapter explains the design of the study, presents the results and discusses them.

6.1 User Study Design and Procedure

While the main goal of the study is to validate the saddle as an input device, the study is actually designed around a different hypothesis with the validation of the saddle as an indirect result of the study. This is because a useful validation would take place both with trained teleoperators and in combination with an upper body input device, as the saddle is designed to improve the whole body control over a robot. Since this is the first functional prototype of the saddle, this would be too early, so the study is rather designed to validate the concept of the saddle. For this, two steering approaches are compared in a simple cross over study: a pure differential steering and a fusion of differential and holonomic steering where sideways driving will be available in addition to the standard movements of a differential steering. The technical setup of the user study can be seen in figure 6.1.

After getting an introduction to the saddle input device and the tasks ahead, basic demographical information is collected from the participants. Each participant goes through the same procedure twice. First there is a three-minute interval during which they can get used to the steering approach and the input device itself. An exemplary course (figure 6.2) is designed where they can steer the image of a robotic platform through a simulated environment. After this training time, they will complete a task (figure 6.3) where they are asked to navigate through the map while matching the targets as quickly as possible while still driving accurately, i.e., without hitting a wall. As an incentive not to drive into the walls, the robot stops for one second if a wall is hit. During the execution of the task both the time needed and the number of contacts with the wall are recorded. After finishing the task, the participants are asked to answer four short questions:

- How successful were you with controlling the robot?
- How confident were you while controlling the robot?

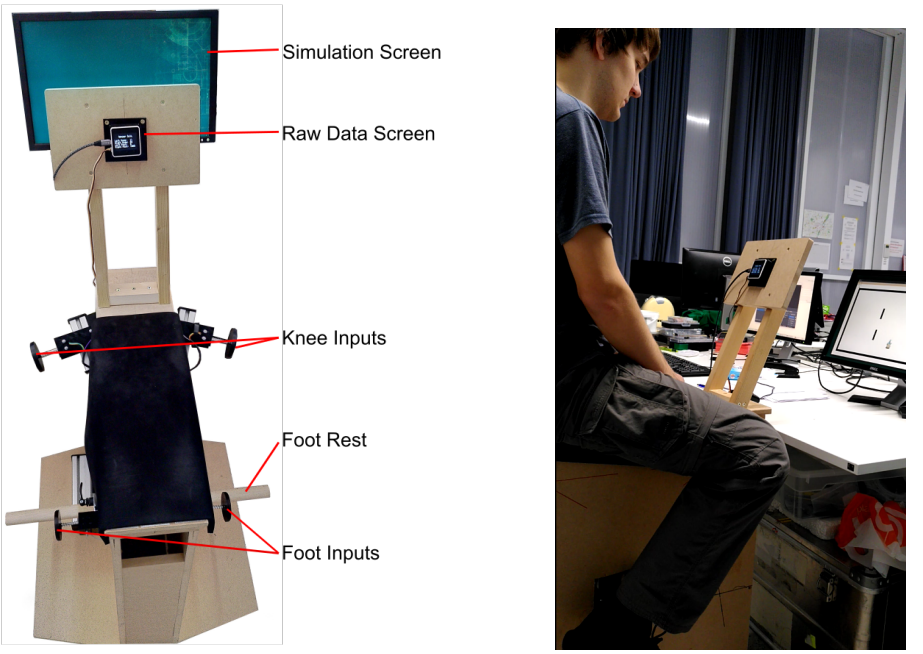

(a) general setup **(b)** example of the study setup in action

Figure 6.1: The technical setup of the user study.

- How intuitive were the controls?
- How good was the overall quality of telerobotic interaction?

Each question is answered on a scale from one to seven. Additionally, they fill out the NASA Task Load Index Questionnaire (Hart and Staveland, 1988), a standardized questionnaire to evaluate how demanding a task is. This procedure is then repeated with the other steering approach. Finally, the participants are asked for final feedback and to choose which steering approach they preferred and why. All documents filled out by the participants can be seen in appendix B.

6.2 Results

The study was conducted with 23 participants (6 females, 17 males). The average age was 27.8 years, with ages ranging from 20 to 41 and a standard deviation of 4.4 years. 17 participants stated their dominant leg was the right, one left and five said neither or both legs were dominant. 14 Participants did not have any experience in teleoperation, nine did, rating themselves at an average experience of 3.7 out of seven. Three participants said they had experience with horseback riding and five with driving a motorcycle. Due to misunderstanding the task one participant (number 19) had to be excluded from the evaluation.

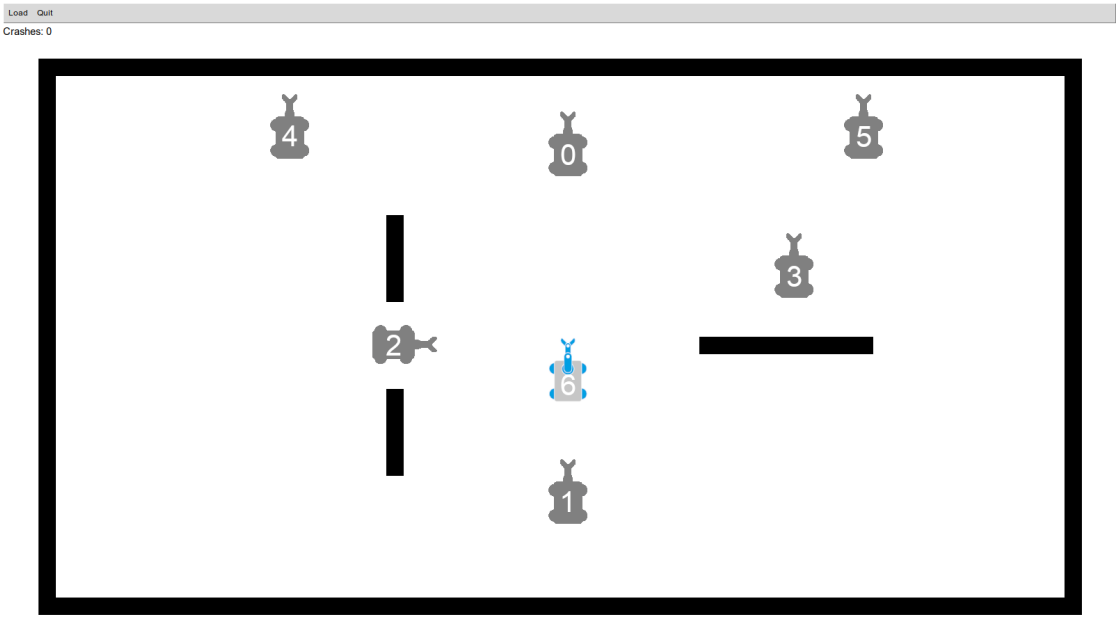

Figure 6.2: This course is used for training. The participants can drive around freely and try to match the targets (which are shown in a loop one at a time). If they drive into the black wall, the robot stops for one second.

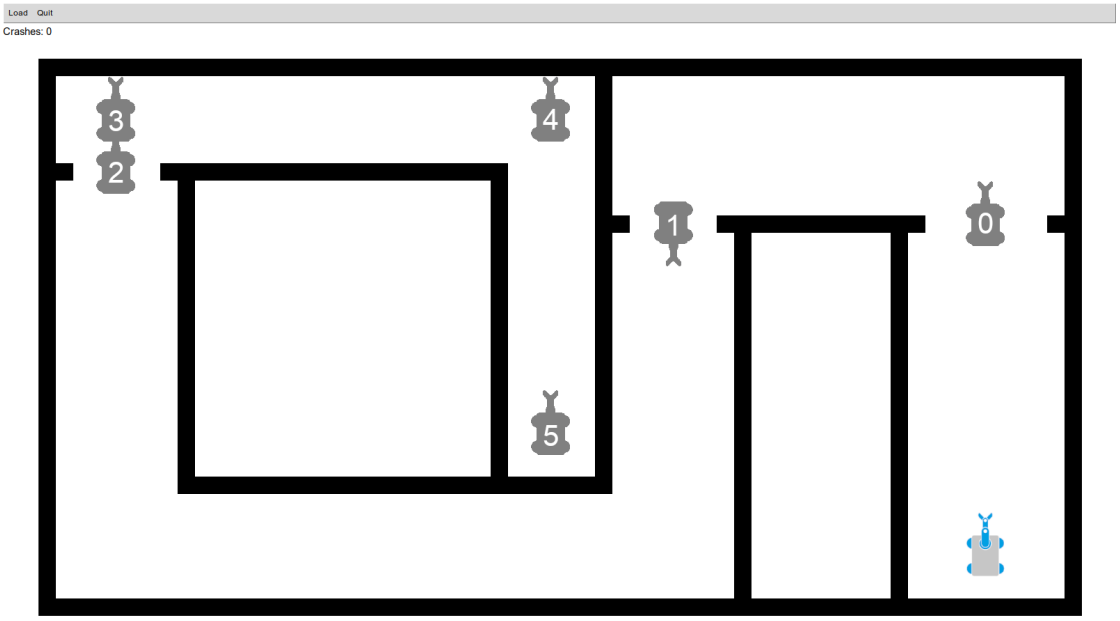

Figure 6.3: This course is used as the task for the study. The participants are asked to navigate through the map while matching the targets (which are shown one at a time) as quickly as possible without hitting the black walls. If they do drive into a wall, the robot stops for one second as a penalty.

6.2.1 Objective Data

The completion time and wall contacts of each participant can be seen in figure 6.4. On average, completing the task with differential steering took $149.8\,\text{s}$ ($\sigma = 46.0\,\text{s}$) and $127.3\,\text{s}$ ($\sigma = 58.9\,\text{s}$) with fused steering, which is a significant difference ($t = 2.3, p < 0.05$). Furthermore, completion times with fused steering were much better when starting with differential steering ($110.8\,\text{s}$ ($\sigma = 49.6\,\text{s}$)) compared to $143.7\,\text{s}$ ($\sigma = 62.9\,\text{s}$) when starting with fused steering. There was no significant difference in wall hits between differential (1.1 hits, $\sigma = 1.7$) and fused steering (1.0 hits, $\sigma = 1.9$).

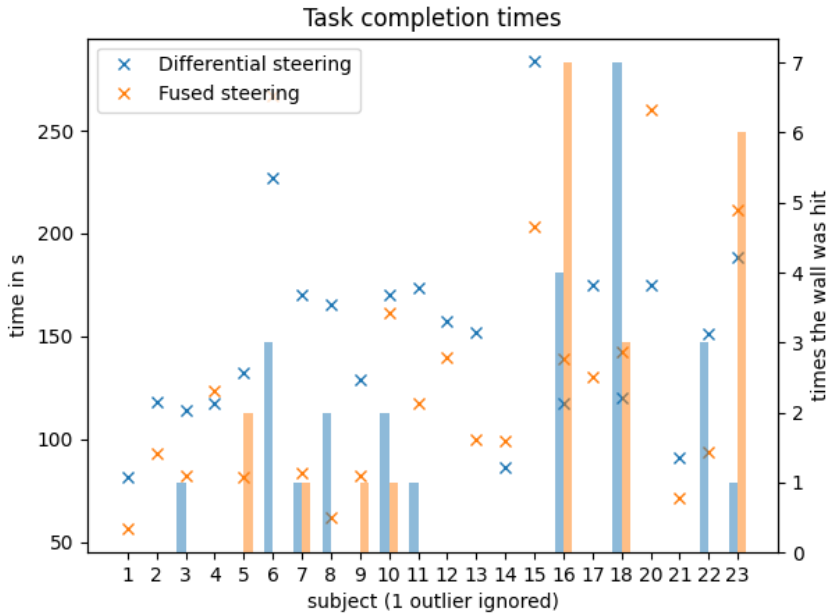

Figure 6.4: This plot shows the completion time (as crosses) and the number of wall contacts (as bars) for each participant. Blue represents the results of the differential steering and orange the fused steering. Odd subject numbers started with the differential steering, even with the fused.

6.2.2 Subjective Data

The result of the post-task questions and the NASA TLX are summarized in table 6.1. Plots individually comparing the different steering modes for each item can be found in appendix C. It can be seen that for all categories but intuition and physical demand a significant difference was found. As for the final feedback, only one participant preferred the differential driving over the fused one because it was closer to the familiar way to drive a car.

Table 6.1: Results of the questions (from one to seven) and the NASA TLX (from zero to 100) answered after each task. It should be noted that while for all the other categories a higher score is considered better, for performance it is the other way around.

	Differential Steering	Fused Steering	Statistical Significance
Success	5.0 (1.1)	5.9 (1.0)	$t = -3.8, p < 0.05$
Confidence	4.8 (1.2)	5.9 (1.1)	$t = -4.8, p < 0.05$
Intuition	5.5 (0.8)	5.9 (1.2)	none
Overall Quality	5.2 (1.1)	5.9 (1.0)	$t = -3.2, p < 0.05$
NASA TLX			
Mental Demand	59.3 (20.4)	43.6 (19.4)	$t = 7.3, p < 0.05$
Physical Demand	46.4 (21.0)	42.5 (19.6)	none
Temporal Demand	48.0 (24.2)	35.5 (19.9)	$t = 3.2, p < 0.05$
Performance	38.0 (20.4)	30.0 (24.8)	$t = 2.2, p < 0.05$
Effort	63.0 (18.4)	44.8 (19.1)	$t = 4.6, p < 0.05$
Frustration	40.2 (24.5)	21.8 (17.9)	$t = 4.3, p < 0.05$

6.3 Discussion of the results

The results show, that adding the ability to drive sideways to a differential steering approach does not make it too complicated but rather improves the steering. Furthermore, the saddle seems to be a valid input device, as nearly all scores of the post-task questions were higher than five out of seven, with the confidence for differential steering being the only one slightly below five. In addition to the presented values, most of the participants also gave mainly positive feedback both to the fused steering approach and the input device. Many noted that while it did need some time getting used to, it turned out to be more intuitive than they expected after the sensor mappings had been explained to them. Most of the criticism was directed towards the placement of the sensors, which could not be ideally adjusted, or the sensors having a tendency of getting stuck.

CHAPTER 7

SUMMARY AND FUTURE WORK

This thesis covered the development process of a saddle equipped with four sensors in order to serve as an input device for teleoperation. On this saddle, the operators use their knees and feet to drive a robotic platform like Justin. After having chosen linear potentiometers as sensors, modules were developed to transfer the movement of the legs to the position of the lever of the potentiometer. Compression springs were integrated into the modules to return the module to zero position when not pressed. Furthermore, a software infrastructure was implemented in which the sensor values are read by an M5Core2 microcontroller and sent to a computer via USB. The values are filtered and interpreted in a simulink model. This model returns movement values that can be used by the control software of a robot or a simulation to move the platform accordingly. Such a simulation was implemented and used in a user study designed to validate the saddle as an input device and compare differential driving with a fusion of differential and holonomic driving. The study showed significantly better results for the fused steering approach in almost all aspects as well as returning positive results and feedback on the saddle as an input device in general.

As can be seen from some of the feedback of the user study, there is still much potential for improving the saddle. One of the most obvious aspects is eliminating the problems with the sensor modules, i.e., improving the guidance and or reducing the friction of the rod to avoid the module getting stuck. Furthermore, the sensor positioning should be analyzed and reevaluated under ergonomic aspects. Possible changes of the concept include evaluating a different positioning of the foot sensors on the saddle base to be used like the gas pedal in a car (see figure 7.1). Alternatively, a sensor measuring rotational changes like a rotary potentiometer could be integrated into the foot rest so that the foot needs to rotate rather than to press. Furthermore, other force sensors than the FSR used could be evaluated as an alternative to the current sensor modules. To make teleoperation with the saddle more transparent, more feedback channels could be added. For example, vibration actuators could be integrated to warn the operator about upcoming collisions. Another idea would be integrating a visual representation of the sensor values and/or the current movement command into the VR headset of the HUG. Since the user study only gave a first impression about the usability of the saddle, it should be compared to alternative input devices, for example the approach of Schwarz et al. or the current situation with the HUG, where the operator needs to choose between driving and controlling the arms. As to the fused steering approach, maybe a way can be found to implement full holonomic driving (including driving diagonally) as well as differential driving, as both approaches have advantages in different scenarios. Before the saddle can be combined with the HUG, another problem needs to be solved: One part of the

Figure 7.1: An alternative placement for the foot sensor on the saddle base to be pressed like a gas pedal in a car rather than with a sideways motion like before.

HUG not considered in the design of the saddle is a three pedal foot switch used for indexing and as a deadman switch to ensure safe operations. As the feet would no longer be free to operate the switch, its functions would need to be integrated elsewhere in the combined input device. For example, the deadman switch could be incorporated by only allowing robotic action if at least one and no more than three of the four sensors are being pressed. That way, operating the arms can be achieved no matter if the platform is moved or not, as pressing only one sensor does not result in driving.

Additionally, the saddle can also be tested for operating other robotic platforms than Justin and EDAN, for example the Light Weight Rover LRU (Wedler et al., 2015) or the Suspended Aerial Manipulator SAM (Sarkisov et al., 2019). Furthermore, as it provides four inputs controlled with the teleoperators legs with freely interchangeable functions, it can also be considered for use as an additional or alternative input device for other use cases of teleoperation. Example use cases include telesurgery (Seibold et al., 2018), the robotic assembly of modular sattelites in earth orbit (Martins et al., 2018) and the on-orbit repair and service of sattelites (Artigas et al., 2016).

APPENDIX A

FINAL HARDWARE

The following shows the final prototype of the saddle from two perspectives (figure A.1). Furthermore, different views of the final sensor module developed in chapter 4 can be seen in figure A.2

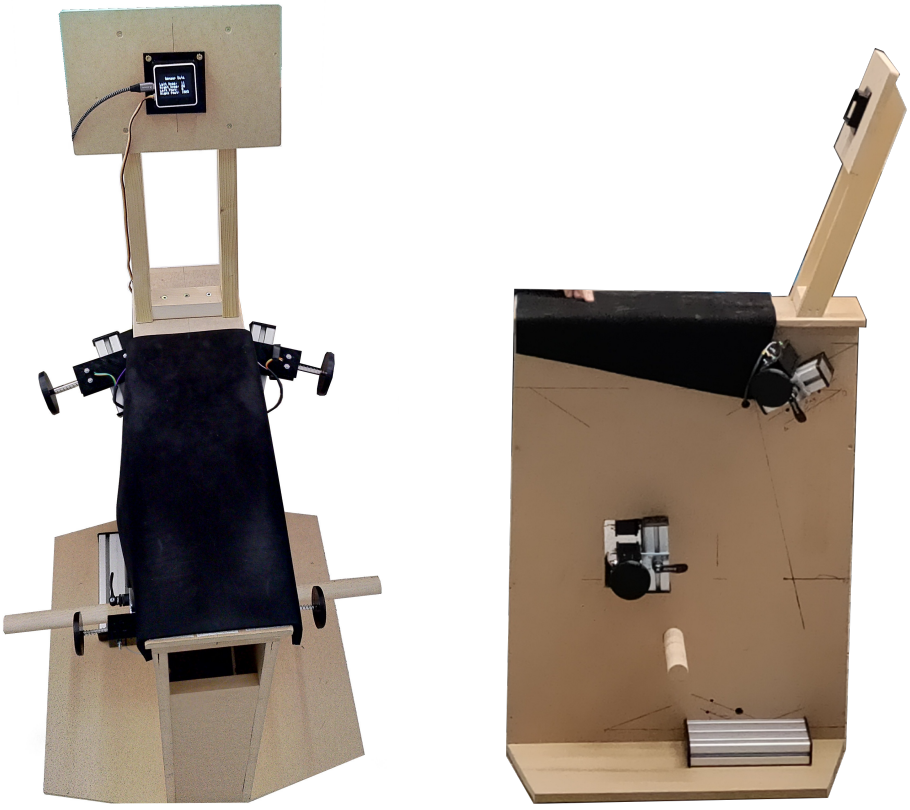

(a) from behind **(b)** from the side

Figure A.1: The final saddle prototype from two different perspectives.

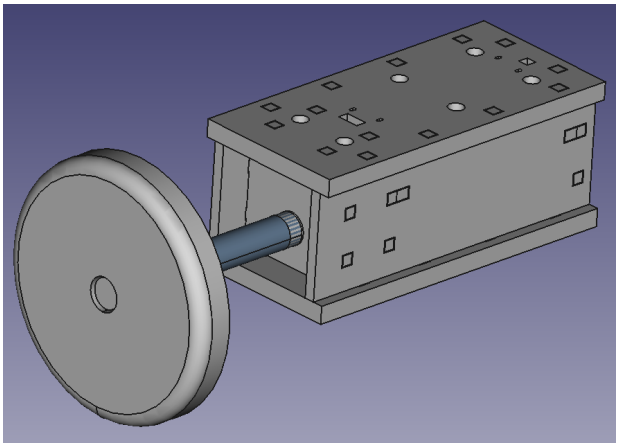

(a) Overview of the final sensor module.

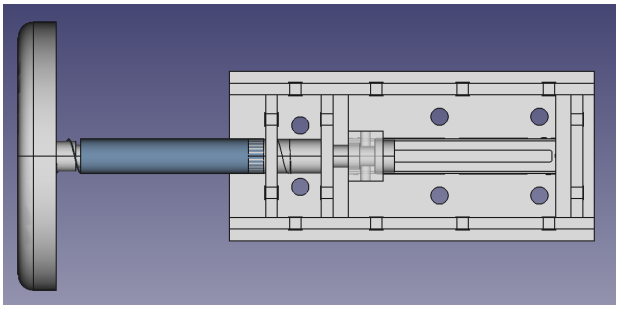

(b) Top view of the sensor module with the top plate removed.

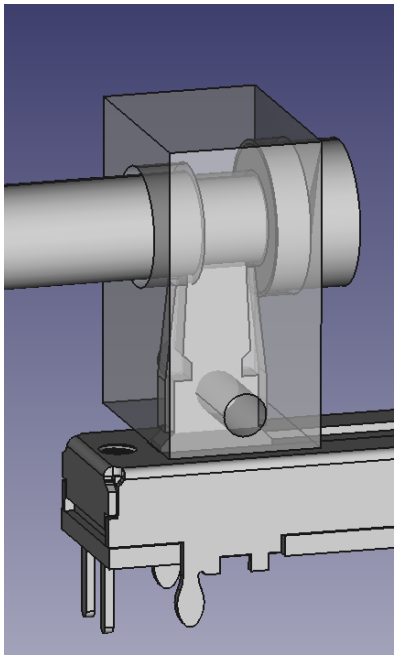

(c) Detailed view of the part connecting the potentiometer's lever and the rod.

Figure A.2: Different views of the CAD model of the final sensor module.

APPENDIX B

USER STUDY DOCUMENTS

In the following, the documents used in the user study (see chapter 6) are shown. The design of the demopgraphic questionnaire (figure B.1) as well as the post-task and post-study questionnaires (figures B.2 and B.4) are based on questionnaires used in previous studies at the Institute of Robotics and Mechatronics of the German Aerospace Center.

SN: _____

Date: _____

Time: _____

Participant Code: ☐☐ ☐☐ ☐☐ ☐☐

First two letters of mother's *first name* | First two letters of father's *first name* | Month of mother's birth | Month of father's birth

Demographic Questionnaire

1. Age: _____

2. Sex: Male ☐ Female ☐ Diverse ☐

3. Dominant Foot: Left ☐ Right ☐ Neither/Both ☐

4. Profession / Occupation: _____

5. Do you have experience with robotic teleoperation applications?

a) No ☐ Yes ☐

b) If yes, how much experience do you have? (cross in the scale)

1 very low	2	3	4	5	6	7 very much

6. Do you have experience with horseback riding? No ☐ Yes ☐

7. Do you have experience with driving a motorcycle? No ☐ Yes ☐

Figure B.1: The demographic questionnaire used in the user study.

SN: _____

Date: _____

Time: _____

Steering:_____

Participant Code: ☐☐ ☐☐ ☐☐ ☐☐

First two letters of mother's *first name* | First two letters of father's *first name* | Month of mother's birth | Month of father's birth

Comparison of steering approaches on a multi-sensoral saddle

1) How successful were you with controlling the robot?

1 not at all	2	3	4	5	6	7 very successful

2) How confident were you while controlling the robot?

1 not at all	2	3	4	5	6	7 very confident

3) How intuitive were the controls?

1 not at all	2	3	4	5	6	7 very intuitive

4) How good was the overall quality of the telerobotic interaction?

1 very bad	2	3	4	5	6	7 very good

Figure B.2: The post-task questionnaire to be filled out after the completion of each task.

Figure 8.6

NASA Task Load Index

Hart and Staveland's NASA Task Load Index (TLX) method assesses work load on five 7-point scales. Increments of high, medium and low estimates for each point result in 21 gradations on the scales.

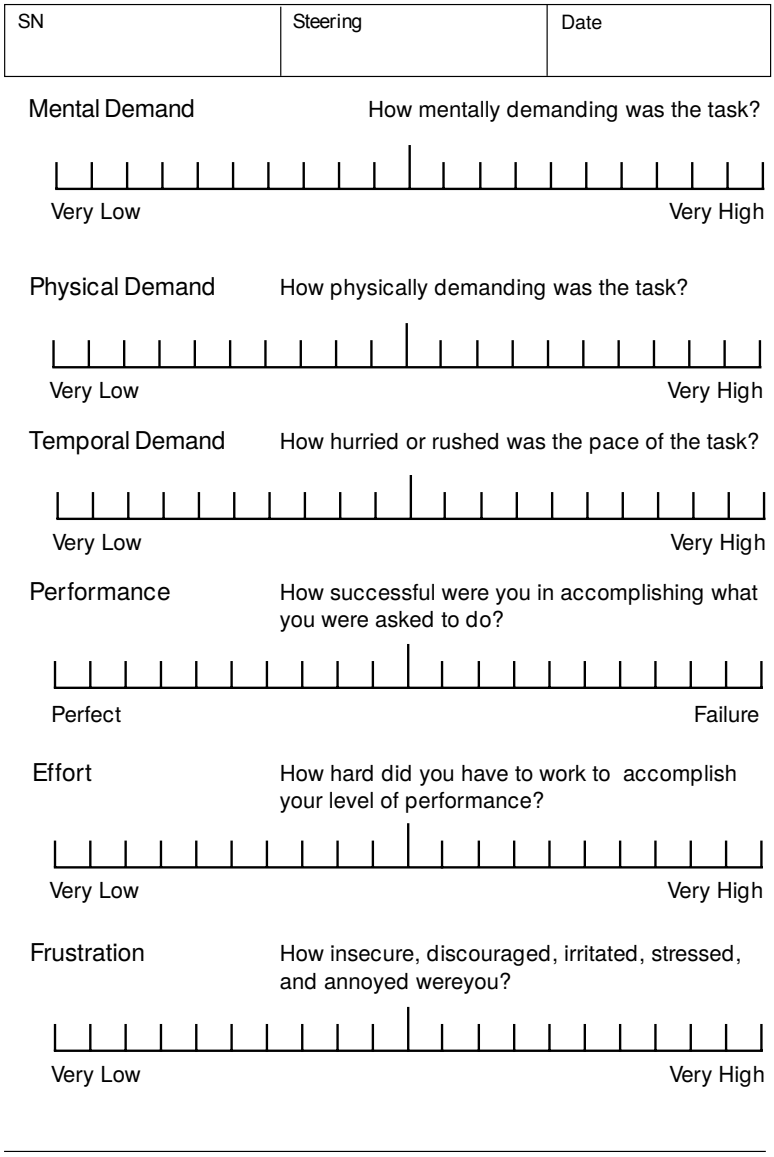

Figure B.3: The NASA Task Load Index questionnaire by Hart and Staveland (Hart and Staveland, 1988) to be filled out after the completion of each task.

SN: _____

Date: _____

Time: _____

Participant Code: ☐☐ ☐☐ ☐☐ ☐☐

First two letters of mother's *first name* | First two letters of father's *first name* | Month of mother's birth | Month of father's birth

Comparison of steering approaches on a multi-sensoral saddle

Final Feedback

1) Which steering condition did you prefer?

a) Sideways driving enabled ☐ Sideways driving disabled ☐

b) Why?

2) Would you like to leave any comments or criticism about the system (including the saddle, sensors, command-bindings and conditions)?

Figure B.4: The post-study questionnaire to be filled out at the end of the study.

APPENDIX C

SUBJECTIVE RESULTS OF THE USER STUDY

In this chapter, plots of the subjective results of the user study (as seen in section 6.2.2) can be found. Figure C.1 shows the results of the post-task questionnaires (which can be seen in figure B.2), whereas figure C.2 shows the results of the NASA TLX (which can be seen in figure B.3).

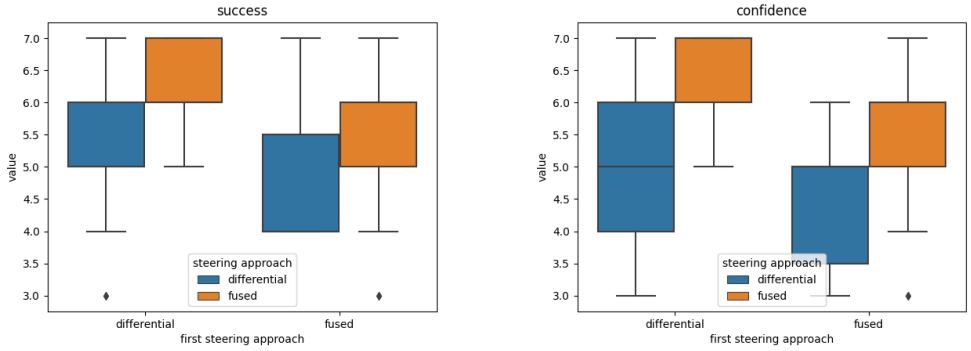

(a) How successful were you with controlling the robot?

(b) How confident were you while controlling the robot?

(c) How intuitive were the controls?

(d) How good was the overall quality of telerobotic interaction?

Figure C.1: The results of the post-task questionnaires (as seen in figure B.2) compared by the initial steering mode. Each question was answered on a scale from one to seven.

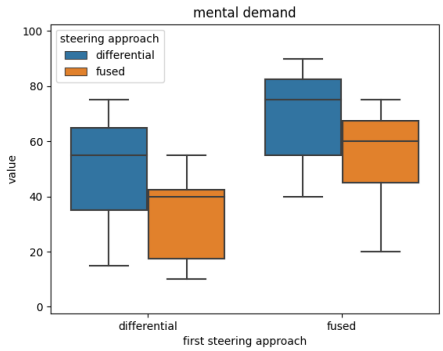

(a) mental demand

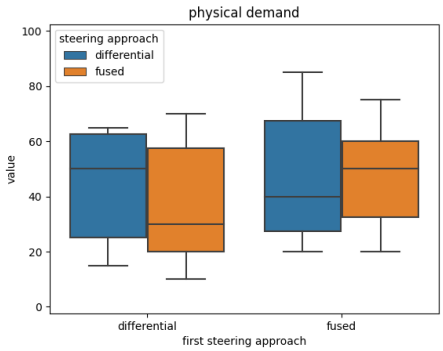

(b) physical demand

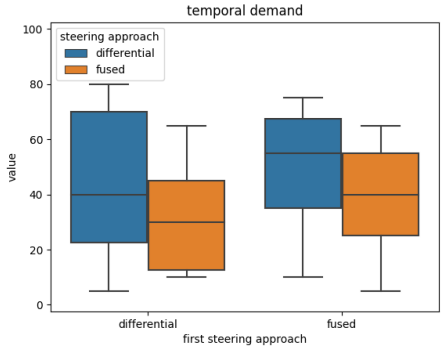

(c) temporal demand

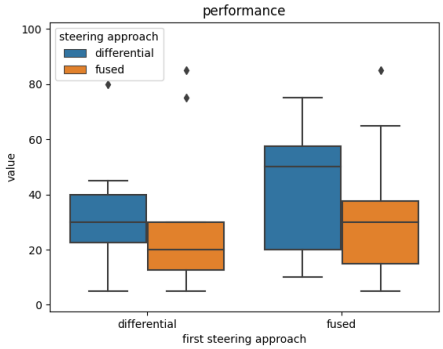

(d) performance

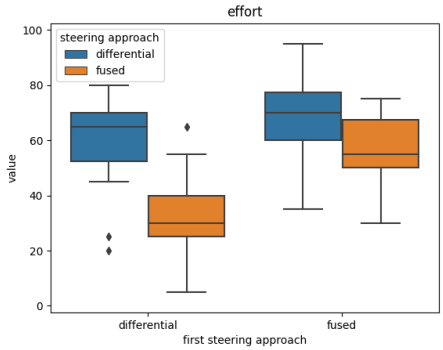

(e) effort

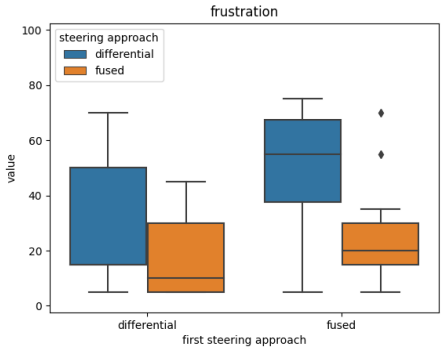

(f) frustration

Figure C.2: The results of the NASA Task Load Index (as seen in figure B.3) compared by the initial steering mode. Each question was answered on a scale from zero to 100. It should be noted that while for all the other categories a higher score is considered better, for performance it is the other way around.

APPENDIX D

DIGITAL APPENDIX

This thesis comes with a digital appendix containing files that, while not necessary for understanding the development process of the input device, can give more insights on some aspects. The digital appendix is structured as follows:

- *cad/*: CAD files of the sensor modules (created in FreeCAD)
- *src/*:
  - *m5_sensordata/*: code running on the M5Core2
  - *robot_saddle_sim/*: robot steering simulation used in the user study
  - *m5_data_publisher.py*: code for publishing received sensor values to LN
  - *m5_interpreter.slx*: simulink model for sensor data processing
  - *saddle_sensor_test.py*: code for testing the sensors on the saddle
- *study/*: the different questionnaires used in the user study
- *video/*: a video where the saddle is used for driving EDAN for the first time

Please note that the code will probably not work outside the Institute of Robotics and Mechatronics of the German Aerospace Center, as most of it depends on LN functionalities proprietary to the institute.

BIBLIOGRAPHY

Artigas, Jordi et al. (2016). "Teleoperation for on-orbit servicing missions through the ASTRA geostationary satellite." In: *2016 IEEE Aerospace Conference*, pp. 1–12. DOI: 10.1109/AERO.2016.7500785.

Bourns (2015). *PTA Series - Low Profile Slide Potentiometer*. Last Access: 05.02.2023. URL: https://www.distrelec.de/Web/Downloads/_t/ds/PTA4543-2015DPB103_eng_tds.pdf.

Ergonomics Standards Committee (2020). *Ergonomics - Human body dimensions - Part 2: Values (DIN33402-2:2020)*. Tech. rep. DIN German Institute for Standardization.

Fuchs, M. et al. (2009). "Rollin' Justin - Design considerations and realization of a mobile platform for a humanoid upper body." In: *2009 IEEE International Conference on Robotics and Automation*, pp. 4131–4137. DOI: 10.1109/ROBOT.2009.5152464.

Gutekunst Spring Factories (2023). *Data sheet Compression spring: D-090G*. Last Access: 05.02.2023. URL: https://www.federnshop.com/en/data-sheet/federnshop-data-sheet-compression-spring_d-090g.pdf.

Hart, SG and LE Staveland (1988). "Development of NASA-TLX (Task Load Index): Results of empirical and theoretical research." In: *P. A. Hancock and N. Meshkati (Eds.) Human Mental Workload*.

Hulin, Thomas et al. (2011). "The DLR bimanual haptic device with optimized workspace." In: *2011 IEEE International Conference on Robotics and Automation*, pp. 3441–3442. DOI: 10.1109/ICRA.2011.5980066.

LaValle, Steven M (2013). *Mobile Robotics - Chapter 2: Movable Machines*. Last Access: 07.02.2023. URL: http://lavalle.pl/mobile/mch2.pdf.

M5Stack (n.d.[a]). *ANGLE*. Last Access: 05.02.2023. URL: https://docs.m5stack.com/en/unit/angle.

– (n.d.[b]). *PbHUB*. Last Access: 05.02.2023. URL: https://docs.m5stack.com/en/unit/pbhub.

– (n.d.[c]). *ToF*. Last Access: 07.02.2023. URL: https://docs.m5stack.com/en/core/core2.

– (n.d.[d]). *ToF*. Last Access: 05.02.2023. URL: https://docs.m5stack.com/en/unit/tof.

– (n.d.[e]). *UNIT FADER*. Last Access: 05.02.2023. URL: https://docs.m5stack.com/en/unit/fader.

– (n.d.[f]). *WEIGHT*. Last Access: 05.02.2023. URL: https://docs.m5stack.com/en/unit/weight.

Martins, Thiago Weber et al. (2018). "Space Factory 4.0 - New processes for the robotic assembly of modular satellites on an in-orbit platform based on "'Industrie 4.0" approach." In: *IAC, 69th International Astronautical Congress*.

Niemeyer, Günter et al. (2016). "Telerobotics." In: *Springer Handbook of Robotics*. Ed. by Bruno Siciliano and Oussama Khatib. Cham: Springer International Publishing, pp. 1085–1108. ISBN: 978-3-319-32552-1. DOI: 10.1007/978-3-319-32552-1_43.

Ohmite (2018). *FSR Series - Force Sensing Resistor*. Last Access: 05.02.2023. URL: https://www.distrelec.de/Web/Downloads/_t/ds/Ohmite_FSR_eng_tds.pdf.

Sarkisov, Yuri S. et al. (2019). "Development of SAM: cable-Suspended Aerial Manipulator." In: *2019 International Conference on Robotics and Automation (ICRA)*, pp. 5323–5329. DOI: 10.1109/ICRA.2019.8793592.

Schwarz, Max et al. (2021). "NimbRo Avatar: Interactive Immersive Telepresence with Force-Feedback Telemanipulation." In: *2021 IEEE/RSJ International Conference on Intelligent Robots and Systems (IROS)*, pp. 5312–5319. DOI: 10.1109/IROS51168.2021.9636191.

Seeed Technology (n.d.). *Grove - 12 bit Magnetic Rotary Position Sensor (AS5600)*. Last Access: 05.02.2023. URL: https://wiki.seeedstudio.com/Grove-12-bit-Magnetic-Rotary-Position-Sensor-AS5600/.

Seibold, Ulrich et al. (2018). "The DLR MiroSurge surgical robotic demonstrator." In: *The Encyclopedia of Medical Robotics*, pp. 111–142. DOI: 10.1142/9789813232266_0005.

TE Connectivity Company (2020). *FX19 - Compression Load Cell*. Last Access: 05.02.2023. URL: https://www.te.com/commerce/DocumentDelivery/DDEController?Action=srchrtrv&DocNm=FX19&DocType=DS&DocLang=English.

Vogel, Jörn, Annette Hagengruber, et al. (2020). "EDAN: An EMG-controlled Daily Assistant to Help People With Physical Disabilities." In: *2020 IEEE/RSJ International Conference on Intelligent Robots and Systems (IROS)*, pp. 4183–4190. DOI: 10.1109/IROS45743.2020.9341156.

Vogel, Jörn, Daniel Leidner, et al. (2021). "An Ecosystem for Heterogeneous Robotic Assistants in Caregiving: Core Functionalities and Use Cases." In: *IEEE Robotics and Automation Magazine* 28.3, pp. 12–28. DOI: 10.1109/MRA.2020.3032142.

Wedler, Armin et al. (2015). "LRU-lightweight rover unit." In: *Proc. of the 13th Symposium on Advanced Space Technologies in Robotics and Automation (ASTRA)*.

Wüstenhoff, Tilo (n.d.). *total hug*. Last Access: 14.02.2023. URL: https://www.dlr.de/rm/Portaldata/52/Resources/projekte_und_andere_forschung/telepraesenz/total_hug_385x576.jpg.

Zeidis, Igor and Klaus Zimmermann (2019). "Dynamics of a four-wheeled mobile robot with Mecanum wheels." In: *ZAMM - Journal of Applied Mathematics and Mechanics / Zeitschrift für Angewandte Mathematik und Mechanik* 99.12, e201900173. DOI: https://doi.org/10.1002/zamm.201900173.

ACKNOWLEDGEMENTS

The author would like to thank Prof. Dr.-Ing. Frank Wallhoff and Dr.-Ing. Thomas Hulin for their great support and supervision. This also includes Tilo Wüstenhoff and Jörn Vogel. Furthermore thanks to the Institute of Robotics and Mechatronics of the German Aerospace Center for the opportunity to conduct this project and for their warm welcome and continuous support.

This work was partially funded by the German Research Foundation (Deutsche Forschungsgemeinschaft, DFG) as part of Germany's Excellence Strategy - EXC 2050/1 - Project ID 390696704 - Cluster of Excellence "Centre for Tactile Internet with Human-in-the-Loop" (CeTI) of Technische Universität Dresden and the Bavarian Ministy of Economic Affairs, Regional Developent and Energy (StMWi) by means of the project SMiLE2gether (LABAY102).

EIGENSTÄNDIGKEITSERKLÄRUNG

Erklärung gemäß §1 (5) Allgemeiner Teil (Teil A) der Prüfungsordnung für die Bachelor-Studiengänge (BPO) an der Jade Hochschule Wilhelmshaven/Oldenburg/Elsfleth in der Fassung vom 21.10.2014 (Verkündungsblatt Nr. 56/2014 der Jade Hochschule)

Diese Bachelorarbeit ist eine Einzelarbeit. Ich erkläre hiermit, diese Bachelorarbeit selbstständig und ohne fremde Hilfe verfasst und keine anderen als die angegebenen Quellen und Hilfsmittel benutzt zu haben.

. . . . . .

Ort, Datum, Unterschrift (Tjark Welter Matr.-Nr. 6032630)

LICENSE